Hyperons Dalitz decays @ HADES

Krzysztof Nowakowski on behalf of the HADES collaboration
Faculty of Physics, Astronomy and Applied Computing Science, Jagiellonian University, krakw, Poland

E-mail: k.nowakowski@doctoral.uj.edu.pl

Abstract. The electromagnetic transition form factors are an ideal tool to discriminate between various models of hadron structure. However, measuring them is a great experimental challenge, especially in time-like region, that is inaccessible by annihilation experiments. The HADES detector is, thanks to ability to identify di-leptons, an ideal tool to perform measurement in the low q^2 time-like region. This gives access to transitions form factors of excited baryon (N*) states, via Dalitz decays ($N^* \to N\gamma^* \to Ne^+e^-$). In this paper I will present a simulation study of a planned experiment, dedicated to measurements of Dalitz decays, produced with a proton beam of kinetic energy $E_k = 4.5$ GeV. In addition, the current status of the analysis of data collected at $E_k = 3.5$ GeV will be reported.

1. Dalitz decays

Information about internal structure of baryons is encoded in quantities called form factors - represented as functions of the four-momentum transfer q^2. There are two distinct, kinematically complementary regions: the time-like (for $q^2 > 0$) and the space-like (for $q^2 < 0$). The time-like part is easily accessible through annihilation experiments (e.g. $e^+e^- \to N\overline{N}$), although kinematics do not allow access to the region $0 < q^2 < 4m_b^2$, m_b being the mass of the produced baryon. On the other hand, this kinematic range is accessible through a process called Dalitz decay, where a baryon undergoes transition into a lighter state by emitting a virtual photon which decay into di-lepton pair ($N^* \to Nl^+l^-$). Here, $q^2 = m_{N^*} - m_N$. In this way, we can perform a direct comparison between the results for time- and space-like regions at $q^2 = 0$. In this reaction, the transition amplitude is modified by a quantity called electromagnetic Transition Form Factor (eTFF). Furthermore, hadron decays are heavily influenced by intermediate vector mesons. The first measurements of HADES indeed reveal the important role of the ρ meson in $\Delta(1232)$ and $N^*(1520)$ decays [1]. The proposed experimental program of hyperon Dalitz decays, described in more details below, extends these studies to strange baryon sector.

2. HADES detector

The **H**igh **A**cceptance **D**i-**E**lectron **S**pectrometer (HADES) [2] is a detector located at the GSI Helmholtzzentrum für Schwerionenforschung. The HADES detector was designed for various measurements with the especial emphasis on di-electron detection. Thanks to versatility of the SIS18 (German: **S**chwer**I**onen**S**ynchrotron) accelerator and a secondary pion beam facility, various kind of experiments can be conducted: starting from pion scattering on proton or nucleus targets, through proton-proton and proton-nucleus reactions, up to the heavy ion collisions.

The detector provides almost full azimuntal angular coverage whereas the acceptance in the polar angle ranges from 18° to 80°. Two sets of Multi-wire Drift Chambers (MDC) together with a superconducting toroid magnet allow for momentum measurements with $\frac{dp}{p} \approx 2-3\%$ and particle identification (PID) via energy loss measurement. The PID is further enhanced by high resolution **T**ime **O**f **F**light (TOF) detectors ($\sigma \approx 80$ ps) and a hadron-blind **R**ing **I**maging **CH**erenkov (RICH) detector. A combined information form the detectors allow for efficient p/π/K/e separation over broad momentum range.

Currently HADES is intensively upgraded to face a new physical program. A brand new **E**lectromagnetic **CAL**orimeter [3, 4] and a new RICH readout system have been already installed and tested during campaign with Ag+Ag collisions. In addition a new **F**or**W**ard **DET**ector [5] will be installed in 2020. It will extend the HADES acceptance to very forward angles, between 0.6° and 7°. This detector will significantly enhance the acceptance for hyperon reconstruction, since momentum conservation causes the proton from Λ decay tend to be emitted at small polar angles.

3. Hyperon Dalitz decays in HADES

Table 1. Estimated cross-sections and count rates obtained during simulation

Y^* production	$pp \to pK^+\Lambda^*$	$pp \to pK^+\Sigma^*$
σ_{tot}	130μb	80 μb
Y^* Dalitz decay	$\Lambda^* \to \Lambda e^+e^-$	$\Sigma^* \to \Sigma e^+e^-$
σ_{Dalitz}	$8.3 \cdot 10^{-3}\mu$b	$7.0 \cdot 10^{-3}\mu$b
ε_{H^*rec}	0.5%	0.5%
Expected count rate		
proton target	34 part/day	
PE target	240 part/day	

An important part of the upgraded HADES physics program, within FAIR Phase 0, are the measurements of hyperon eTFF. The eTFF can be accessed via measurements of the Dalitz decay Y(hyperon) $\to \Lambda e^+e^-$, where Y refers to a neutral hyperon. The experiments will be performed with the maximal achievable beam energy of the SIS18, $E_k^{max} = 4.5$ Gev. To get an estimate of the expected count rates in the updated HADES detector, a full-scale simulation study was performed at this energy. The investigation demonstrated the importance of the forward tracker, which increases the reconstructed efficiency approximately 50%. Benchmark channels, including excited hyperon states ($\Lambda(1520), \Lambda(1405), \Sigma(1385)$), were simulated together with dominant background channels. Details concerning signal channels are presented in Table 1. The production cross-sections have been estimated based on existing experimental data [6, 7]. Since no electromagnetic Dalitz decay has ever been measured, the branching ratios used in the simulations were obtained by scaling radiative decays $\Lambda(1520)/\Sigma(1385) \to \gamma\Lambda$ measured by the CLAS experiment [8]. A detailed list of simulated background channels is presented in Ref. [9].

The analysis consist of two parts: reconstruction of $\Lambda \to p\pi^-$ decay, and di-lepton identification. Thanks to the relatively long Λ lifetime ($c\tau = 7.89$ cm [10]) it is possible to distinguish the Λ hyperon from other particles by topological cuts. The selection procedure is based on set of geometrical cuts, which separate the Λ displaced decay vertex from the primary vertex. In the simulation only three of them have been used: i) the minimal distance between p and π^- track, is required to be < 20 mm and ii) the Λ decay vertex, reconstructed as a point of closest approach between p and π^-, must be displaced with respect to the target by at least 5 mm along beam line iii) the leptonic tracks were required to match rings registered by the RICH detector. The last criterion strongly suppresses pionic background. To reject e^+e^- pairs from external photo-conversion, the opening angle between the lepton tracks is required to be larger then 4 degrees. Since the background is strongly dominated by the π^0 Dalitz decay, all

di-lepton pairs with $M^{inv}_{e^+e^-} < 140$ MeV were rejected. However, some channels contain more than one di-lepton source, for example events with a hyperon Dalitz decay and a π^0 Dalitz decay. Combinations of particles from two sources leads to combinatorial background. The amount of e^+e^- background can be estimated base on the number of same-sign pairs, according to the formula $N_{e^+e^-} = 2\sqrt{N_{e^+e^+} \cdot N_{e^-e^-}}$.

Final $M^{inv}_{p\pi^-e^+e^-}$ and $M^{inv}_{e^+e^-}$ spectra, representing an equivalent of 4 weeks beam-time, are shown in Fig. 1. The pictures shows that taking into account listed background sources, HADES is able to distinguish between $\Lambda(1520)$ and $\Sigma(1385)$ Dalitz decays. Furthermore, the expected combinatorial background in the experiment is under control.

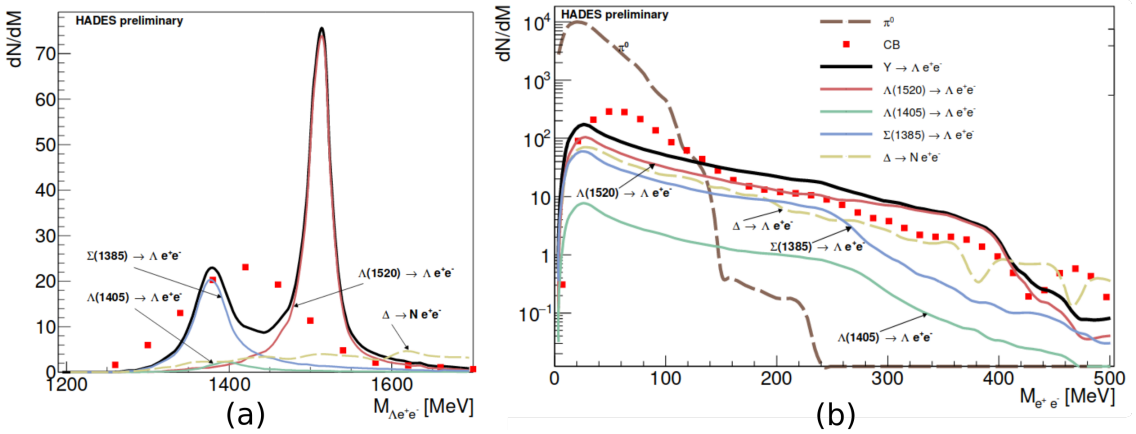

Figure 1. The final results of the simulation. Panel (a): A $M^{inv}_{\Lambda e^+e^-e}$ spectrum. Solid lines represent signal from hyperon Dalitz decays after geometrical cuts and $M_{e^+e^-} > M_{\pi^0}$. Red dots represent combinatorial background, mostly caused by mixing leptons from π^0 decays and Dalitz decays. Panel (b): The expected $M^{inv}_{e^+e^-e}$ spectrum. Below 140 MeV, the signal is dominated by π^0 decays.

4. Analysis of a data collected in previous experiments

Since there are no inclusive cross-sections of $\Lambda(1520)$ and $\Sigma(1385)$ measured for pp at $E_k = 4.5$ GeV, estimates based on inclusive cross section for Λ production [7] and the ratio $\frac{\sigma_\Lambda}{\sigma_\Sigma}$ obtained from hyperon production in pp reaction [11], were used. The cross sections for excited hyperons states for $E_k = 4.5$ GeV are constrained by the analysis of pp collisions at 3.5 GeV. In addition, already existing data sets provides an opportunity to develop a new methodes for the reconstraction of hyperon decays. Because of very low expected BR for radiative decays [8], the hadronic channels were investigated: $\Lambda(1520) \to \pi^+\pi^-\Lambda$ and $\Sigma(1385) \to \pi\Lambda$ (for the latter, see [12]). The main aim of the analysis is to extract inclusive cross sections for hyperon production.

Both decays are two-step processes: in the first step, the excited hyperon decays into ground-state Λ by emitting one or two pions. After propagating a few centimeters, the Λ hyperon decays into $p\pi^-$. One of the most prominent $\Lambda(1520)$ decay channels (BR$\approx 3\%$) is two-pion emission. The decay topology is similar to the Dalitz decay: π^+, π^- and Λ are emitted from the primary vertex, whereas the $\Lambda \to p\pi^-$ decay occures in a secondary vertex.

4.1. Λ reconstruction

The first stage of the inclusive analysis is to reconstruct the Λ hyperon. In the previous analysis done by HADES Λ hyperon was reconstructed by set of geometrical cuts. In this analysis, neural networks (NN) have been applied to reject background using set of variables characterizing the

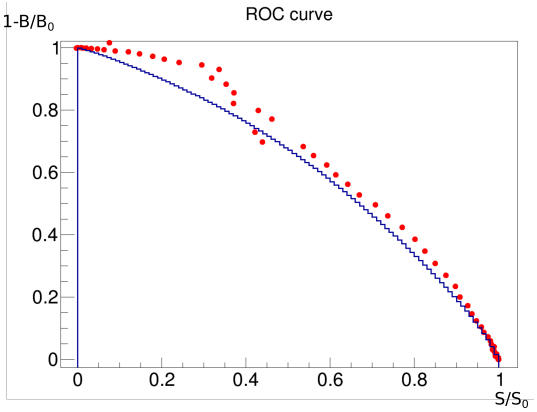

Figure 2. The ROC curve reconstructed from two sources. The blue histogram comes from training and represents ability to distinguish between sets A and A' (see text). The red dots represent the network evaluation on real data.

decay topology. The main advantage of the NN is the ability to find nonlinear correlations between input variables. Almost all geometrical variables such as the point of the closest approach, the minimal distance between tracks, the minimal distance between vertices, are non-linear combinations of variables reconstructed in detector, such as azimuntal and polar angles.

Following the method described in Ref. [13] we trained a classifier without preparing simulated signal and background samples. Instead, the training of the NNs is based on two sets of experimental data: A and A', each containing mixture of background (B) and signal (S) events. Provided the signal-to-background ratio is different in these two sets, the optimal classifier between A and A' is equivalent of the optimal classifier between B ans S.

Thanks to the small Λ width, it is straight-forward to divide the sample into two sets, inside and outside the Λ peak of the π^-p invariant mass spectrum. The ratio between the number of Λ candidates and the number of background events in these two areas are clearly different. However, thanks to thesmall Λ width, the kinematic properties of events in A and A' are similar. Hence, these two regions were used as A and A' data sets. After traning, using a model provided by the TMVA [14] package the final classifier was obtained. From the wide spectrum of available models, the simplest neural network, called a Multi Layer Perceptron (MLP), was used. The MLP consist of certain amount of dense layers, where each neuron from layer N+1 is connected with all outputs from layer N. In this work, the 4 layer network was used. Each layer consists of 23 neurons. The network was used to replace a set of the geometrical cuts, thus only geometrical properties such as distances between tracks and vertex positions were used as an input variables.

The network performance is graphically represented by the **R**eceiver **O**perating **C**haracteristic (ROC) curve. The network output is a number in between 0 and 1. The user has to decide him- or herself at which value of the NN output the signal is considered separated from the background. This value is called the working point. Each point on the ROC curve represents some working point of the network: the signal efficiency (S_{eff}) for this working point and a background rejection ($1 - B_{eff}$). For a perfect classifier, the area under the ROC curve is equal to 1. This means that for each working point, all background events are rejected and the signal efficiency is always 100%.

Thanks to the clearly identifiable Λ mass peak in the data, it was possible to evaluate the classifier signal efficiency Λ_{eff} as a function of the network working point. For each cut on the NN output, a function consisting of a Voight function (signal) folded by a 5th degree polynomial (background) was fitted to the data. The ratio between the number of Λ candidates before and

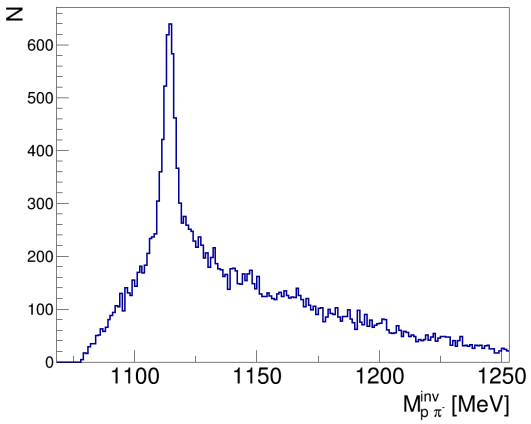

Figure 3. The $\pi^- p$ invariant mass spectrum after selection by the NN. The working point of the network was set to maximize the signal significance, which was found to be 85. In the peak, we we observe 2700 events, which corresponds to the number of Λ hyperons reconstructed in detector.

after the cut on the NN output is defined as the signal efficiency (S_{eff}) for the network. In the same way, it is possible to calculate a background efficiency (B_{eff}) for the network. Then we can compare the ROC curve obtained from the training process (separation between A and A') and from using the trained model on data (separation between B and S). As shown in Figure 2, the efficiency estimated during the training is in very good agreement with real data. This serves as a proof of principle, demonstrating that this data-driven method can be applied to HADES data.

An optimal cut value on the NN output was obtained by comparing the significance of the Λ peak for different working points (see Figure 3). Data samples containing Λ candidates can be used for further analysis including hadronic and leptonic decays of the $\Lambda(1520)$ hyperon.

5. Summary

In this proceedings, I have demonstrated the feasibility of Dalitz decays studies with the upgraded HADES detector. Thanks to already collected data, new analysis methods can be tested. Among these, neural networks combined with a data-driven approach show promising results.

Acknowledgments

Following article has been created thanks to the support by National Science Center by grant PRELDIUM 2017/25/N/ST2/00580.

[1] Adamczewski-Musch J *et al.* (HADES Collaboration) 2017 *Phys. Rev. C* **95**(6) 065205
[2] Agakishiev G *et al.* (HADES collaboration) 2009 *EPJ* **A41** 243–277 (*Preprint* 0902.3478)
[3] Petr H 2020 *Journal of Physics: Conference Series* **this volume**
[4] Arseniy S 2020 *Journal of Physics: Conference Series* **this volume**
[5] Akshay M 2020 *Journal of Physics: Conference Series* **this volume**
[6] Hhler G 1983 *Landolt-Brnstein - Group I Elementary Particles, Nuclei and Atoms* pp 7–8
[7] Adamczewski-Musch J *et al.* (HADES Collaboration) 2017 *PHYSICAL REVIEW C* **95** ISSN 2469-9985
[8] Taylor S, Mutchler G S *et al.* (CLAS Collaboration) 2005 *Phys. Rev. C* **71**(5) 054609
[9] Nowakowski K and Kuboś J 2019 *EPJ Web Conf.* **199** 03011
[10] Olive K A *et al.* (Particle Data Group) 2014 *Chin. Phys.* **C38** 090001
[11] Adamczewski-Musch J *et al.* (HADES collaboration) 2018 *PHYSICS LETTERS B* **781** 735–740 ISSN 0370-2693

[12] Joanna K 2020 *Journal of Physics: Conference Series* **this volume**
[13] Metodiev E M, Nachman B and Thaler J 2017 *Journal of High Energy Physics* **2017** 174 ISSN 1029-8479
[14] Hoecker A, Speckmayer P, Stelzer J, Therhaag J, von Toerne E and Voss H 2007 *PoS* **ACAT** 040 (*Preprint* `physics/0703039`)